



Semianalytical model for simulation of electronic properties of narrow-gap strained semiconductor quantum nanostructures

Jacky Even, François Doré, Charles Cornet, Laurent Pedesseau

► To cite this version:

Jacky Even, François Doré, Charles Cornet, Laurent Pedesseau. Semianalytical model for simulation of electronic properties of narrow-gap strained semiconductor quantum nanostructures. *Physical Review B: Condensed Matter and Materials Physics* (1998-2015), 2008, 77, pp.085305. 10.1103/PhysRevB.77.085305 . hal-00492285

HAL Id: hal-00492285

<https://hal.science/hal-00492285>

Submitted on 15 Jun 2010

HAL is a multi-disciplinary open access archive for the deposit and dissemination of scientific research documents, whether they are published or not. The documents may come from teaching and research institutions in France or abroad, or from public or private research centers.

L'archive ouverte pluridisciplinaire **HAL**, est destinée au dépôt et à la diffusion de documents scientifiques de niveau recherche, publiés ou non, émanant des établissements d'enseignement et de recherche français ou étrangers, des laboratoires publics ou privés.

Semi-analytical model for the simulation of the electronic properties of narrow gap strained semiconductor quantum nanostructures

J. Even, F. Doré, C. Cornet and L. Pedesseau

FOTON-INSA Laboratory, UMR 6082 au CNRS, INSA de Rennes, 20 Avenue des Buttes de Coësmes, CS 14315, 35043 Rennes Cedex, France

Corresponding author: jacky.even@insa-rennes.fr (J. Even)

Abstract.

A complete semi-analytical model is proposed for the simulation of the electronic, mechanical and piezoelectric properties of narrow gap strained semiconductor quantum nanostructures. A transverse isotropic approximation for the strain and a new axial approximation for the strained 8x8 Hamiltonian are proposed. It is applied extensively to the case of InAs/InP quantum dots (QD). Symmetry analysis shows that the non-vanishing splitting of the electron P states is smaller in InAs/GaAs QD than in InAs/InP QD. Analytic expressions for the first and second order piezoelectric polarizations are proposed.

P.A.C.S. 71.20.Nr, 73.21.La, 78.20.Hp

The eight-band k.p model of strained zinc-blende crystals [1] has now been extensively used to describe the electronic structure of III-V semiconductor nanostructures. The eight-band k.p Hamiltonian for bulk strained materials is known [2] to exhibit a two-fold degenerate spectrum related to a diagonalization into two 4x4 blocks exhibiting a dependence on the k-vector. A unitary transformation of this kind, but independent on the tranverse k-vector, has been introduced to transform the 6x6 Hamiltonian in quantum wells (QW) into two 3x3 blocks [3] and more recently [4] to transform the 8x8 Hamiltonian (two 4x4 blocks) for type-II interband cascade lasers. The same approximation was used for cylindrical quantum wires (QWr) [5,6]. The Hamiltonian is block diagonal with the use of a new basis. For the simulation of the electronic properties of quantum dots (QD), the k.p method [7-9] is more or less a standard method although more elaborate theoretical schemes can be employed [10]. The strained-dependent 6x6 Hamiltonian for the valence band in InP/In_{0.49}Ga_{0.51}P QD was simplified into an axially symmetric form in ref. 11. We propose in the present work to extend these approaches to the 8x8 Hamiltonian in order to provide a fast and easy method [12] to evaluate the electronic spectra of narrow-gap semiconductor QDs. Strain effects are taken carefully into account. A new axial approximation is proposed for the strained part of the 8x8 Hamiltonian and applied to InAs/InP and InAs/GaAs QD.

We will consider in this paper QD geometries corresponding to the $C_{\infty v}$ symmetry (around the z axis). The real calculation is performed in 2D cylindrical coordinates (\mathbf{r}, z) on truncated cones of various heights. The chosen dimensions are 8.8nm for the cone height and 35nm for the diameter [9]. Our previous results on InAs/InP QD were obtained either using a complete 3D 8-band k.p strained Hamiltonian [9] or a simple 1-band k.p Hamiltonian with strain renormalized constants in 2D cylindrical coordinates [13]. We may notice that InAs QD grown either on (100) or (311)B misoriented surface are interesting for applications purposes[14,15]. The present model is however expected to be applied only to QD grown on

(100) with cylindrical symmetry. InAs/GaAs QD are finally considered for comparison purposes.

We start from the 8x8 strained Hamiltonian for bulk materials given in ref. 1 or 8. When considering first the unstrained part of the Hamiltonian, the axial approximation is the same as for the 6x6 bulk Hamiltonian [3,11] :

$$R = -\sqrt{3} \frac{\hbar^2}{2m_0} [\gamma_2 (k_x^2 - k_y^2) - 2i\gamma_3 k_x k_y] \approx -\sqrt{3} \frac{\hbar^2}{2m_0} \bar{\gamma} k_-^2 .$$

The other terms of the Hamiltonian can be expressed as a function of the k_z and k_{\pm} operators, without any more approximations for S , P and Q . To extend the model used in

ref. [3,11] to the 8x8 QD Hamiltonian, we introduce : $U = \frac{1}{2\sqrt{3}} \frac{\hbar^2}{2m_0} (P_o k_z + k_z P_o)$,

$$V = \frac{1}{2\sqrt{6}} \frac{\hbar^2}{2m_0} (P_o k_- + k_- P_o) \text{ and } A = E_c + \frac{\hbar^2}{2m_0} \left(\frac{k_- k_+ + k_+ k_-}{2} + k_z k_z \right).$$
 By analogy to QWr

[5,6], it is straightforward to check that the 8x8 QD Hamiltonian is block diagonal in a F_z

basis, where $F_z = J_z + L_z$ is the total angular momentum. Thus, F_z becomes a good quantum

number (each block corresponds to one F_z value). The basis is constructed in a product form

$|J, J_z\rangle |L_z = F_z - J_z\rangle$ where the first term corresponds to the band-edge Bloch functions (the

(u_1, u_2) , (u_4, u_5) , (u_3, u_6) , (u_7, u_8) bands are respectively related to the conduction band

(CB), heavy holes (HH), light holes (LH) and split-off bands (SO)) [13]. The second term

$|L_z = F_z - J_z\rangle$ corresponds to the envelope functions adapted to the usual 1-band cylindrical

representation ($C_{\infty v}$ symmetry). $L_z = 0, \pm 1, \pm 2, \dots$ are related to the so-called S, P, D, ...radial

functions of this representation [13]. All monoelectronic states are a mixing of 8 bands but

we will still indicate, if possible, the most important component (for example "CB 1-S" for

the CB ground state). The boundary conditions are of Neuman type for the S-like radial

functions and of the Dirichlet type for all the other radial functions [12].

This new basis is interesting for several reasons. The state degeneracy is automatically taken into account with F_z and $-F_z$. It is also possible to obtain a schematic electronic spectrum, based only on symmetry considerations. Figure 1 is a comparison between the CB a) and valence band (VB) b) states close to the band gap, in the 1-band representation on the left and in the axial 8-band representation on the right. The CB ground state is mainly associated to $F_z = \pm 1/2$ and to the u_1 or u_2 band-edge Bloch functions and the first S-like envelope functions. The VB ground state is “HH 1S” with $F_z = \pm 3/2$. The electronic gap is then obtained after two separate calculations with $F_z = \pm 1/2$ and $F_z = \pm 3/2$. Another important result is that the degeneracies of CB and VB first excited states (“CB 1P” and “HH 1P”) are lifted by the coupling to remote bands. The same result was obtained for QD with C_{4v} geometry [16]. It is not related to atomistic, strain or piezoelectric effects [10] but simply to the fact that the symmetry of the system in the 8-band description is represented by the F_z quantum number instead of the irreducible representations of the $C_{\infty v}$ symmetry group.

If the strain field is calculated using a continuum mechanical model (elasticity), the axial approximation (symmetry reduction from C_{4v} to $C_{\infty v}$) consists in defining an effective modulus \bar{C} , then $C'_{11} = C'_{22} = \frac{C_{11} + C_{12}}{2} + \bar{C}$, $C'_{12} = \frac{C_{11} + C_{12}}{2} - \bar{C}$ and $C'_{66} = \bar{C}$. This type of material is usually called “transverse isotropic”. Notice that this approximation is much less restrictive than the “full isotropic” approximation usually proposed [11] (for the rest of the paper, $\bar{C} = \frac{C_{11} - C_{12}}{2}$). Our new proposition is also to use the components of strain tensor

$\epsilon_{rr}, \epsilon_{\phi\phi}, \epsilon_{zz}, \epsilon_{rz}$ adapted to cylindrical coordinates (r, ϕ, z) instead of cartesian ones:

$$\epsilon_{xx} = \cos^2(\phi)\epsilon_{rr} + \sin^2(\phi)\epsilon_{\phi\phi}, \quad \epsilon_{yy} = \sin^2(\phi)\epsilon_{rr} + \cos^2(\phi)\epsilon_{\phi\phi}, \quad \epsilon_{xz} = \cos(\phi)\epsilon_{rz},$$

$$\epsilon_{yz} = \sin(\phi)\epsilon_{rz}, \quad \epsilon_{xy} = \frac{\sin(2\phi)}{2}(\epsilon_{rr} - \epsilon_{\phi\phi}).$$

When considering now the strained part of the 8x8

bulk Hamiltonian [1], we propose also to introduce a new axial approximation. This approximation will be applied for the R_ϵ term by analogy to the unstrained Hamiltonian :

$$R_\epsilon = \frac{b\sqrt{3}}{2}(\epsilon_{rr} - \epsilon_{\phi\phi})\cos(2\varphi) - i\frac{d}{2}(\epsilon_{rr} - \epsilon_{\phi\phi})\sin(2\varphi). \text{ In order to keep the } 8 \times 8 \text{ Hamiltonian}$$

in a block diagonal, we propose to replace in \mathbf{R}_ϵ only, the coefficients containing the shear

deformation potentials b and d by a mean value $\frac{\bar{b}\sqrt{3}}{2} = \frac{1}{2}\left(\frac{b\sqrt{3}}{2} + \frac{d}{2}\right) :$

$$R_\epsilon \approx \frac{\bar{b}\sqrt{3}}{2}(\epsilon_{rr} - \epsilon_{\phi\phi})e^{-i2\varphi}. \text{ This approximation is reasonable for the semiconductors}$$

considered in this study since these parameters are for InAs, $\frac{b\sqrt{3}}{2} = -1.58\text{eV}$, $\frac{d}{2} = -1.80\text{eV}$,

for InP, $\frac{b\sqrt{3}}{2} = -1.73\text{eV}$, $\frac{d}{2} = -2.50\text{eV}$, and for GaAs, $\frac{b\sqrt{3}}{2} = -1.56\text{eV}$, $\frac{d}{2} = -2.25\text{eV}$. The

other components of the strained Hamiltonian can be given in cylindrical coordinates without adding any more approximations :

$$S_\epsilon = -d\epsilon_{rz}e^{-i\varphi}, A_\epsilon = a_c(\epsilon_{rr} + \epsilon_{\phi\phi} + \epsilon_{zz}), P_\epsilon = a_v(\epsilon_{rr} + \epsilon_{\phi\phi} + \epsilon_{zz}), Q_\epsilon = b\left(\epsilon_{zz} - \frac{\epsilon_{rr} + \epsilon_{\phi\phi}}{2}\right)$$

$$U_\epsilon = \frac{-P_o}{\sqrt{3}}\frac{\hbar^2}{2m_0}(k_z\epsilon_{zz} + k_t\epsilon_{rz}), V_\epsilon = -\frac{I}{\sqrt{6}}\frac{\hbar^2}{2m_0}(P_o k_- \epsilon_{rr} + P_o k_z \epsilon_{rz} e^{-i\varphi})$$

Figure 2-a shows the variation of gap energy as a function of the truncation height (TH) for InAs/InP QD. A continuous decrease of the energy gap is predicted in good agreement with our previous full-3D study [9] and experimental results [13,14]. The variation of hydrostatic strain $\epsilon_{hydro} = \epsilon_{rr} + \epsilon_{\phi\phi} + \epsilon_{zz}$ (dotted line) and biaxial strain $\epsilon_{biaxial} = \epsilon_{rr} + \epsilon_{\phi\phi} - 2\epsilon_{zz}$ (straight line) is represented for a vertical line passing through the center of a full cone. It indicates that the confining potentials (hydrostatic strain) for HH and CB are almost constant inside the

conic QD, whereas LH potential is stabilized at the top of the cone thanks to the inverted biaxial strain [9].

The variation of the “CB 1S” ($F_z=\pm 1/2$)-“CB 1P” ($F_z=\pm 1/2$ or $F_z=\pm 3/2$) and “HH 1S”-“HH 1P” ($F_z=\pm 1/2$ or $F_z=\pm 5/2$) energy gaps are reported on figure 3-a (the average values are considered for the first CB and HH excited states). A continuous increase of the energy difference between ground state and excited state is predicted for the CB with increasing TH. Indeed, the average radius is decreasing when increasing the TH for the chosen cone. In the VB band a maximum is reached for a TH equal to about 5nm. These results are also in good agreement with our previous work [9], where the energy difference between ground and excited state has been attributed to QD radius, although no systematic study of this property was performed. When the TH is increased, coupling between HH and LH bands (related to the gap increasing (figure 2-a) and the biaxial strain inversion figure 2-b) becomes more important than the effect of the average radius.

Figure 3-b shows the variation of the CB first excited state splitting $E_{F_z=\pm 3/2} - E_{F_z=\pm 1/2}$ (“1P splitting for electrons”) as a function of the TH. This splitting remains very small (less than 1meV) and is related to the couplings of the “CB 1P” excited states to VB states, mainly HH states. This “1P-electrons” splitting increases as the energy gap decreases. In the case of the VB, the first excited state splitting $E_{F_z=\pm 1/2} - E_{F_z=\pm 5/2}$ (“1P splitting for holes”) remains small and changes sign for a TH on the order of 5nm. This is again associated to the strong increase of the HH-LH coupling.

We finally propose (figure 4) a comparison between the InAs/InP and the InAs/GaAs system with the same QD geometry (TH=2.9nm). Due to the larger lattice mismatch in the InAs/GaAs case, a larger energy gap is found (0.90 eV for InAs/GaAs, and 0.78 eV for InAs/InP). The same trend is observed for the calculated “CB 1S”-“CB 1P” (30.6meV for InAs/GaAs and 26.2meV for InAs/InP) and “HH 1S”-“HH 1P” (19.7meV for InAs/GaAs and

16.2meV for InAs/InP) energy gaps. As a result, the CB $E_{F_z=\pm 3/2} - E_{F_z=\pm 1/2}$ (0.14meV for InAs/GaAs and 0.27meV for InAs/InP) and VB $E_{F_z=\pm 1/2} - E_{F_z=\pm 5/2}$ (0.85meV for InAs/GaAs and 0.95meV for InAs/InP) splittings are smaller for the InAs/GaAs QD. Figure 4-a and figure 4-b represents respectively the isodensity surfaces containing 75% of the total density for the $F_z = \pm 1/2$ CB ground state and the $F_z = \pm 1/2$ CB first excited state (the difference with the CB $F_z = \pm 3/2$ first excited state is very small). It is straightforward to check that the spatial distribution of the electronic density has a cylindrical symmetry which is awaited for QD geometries corresponding to the $C_{\infty v}$ symmetry. It is possible to introduce a symmetry breaking by simulating the influence of the piezoelectric potential. Within our axial model, the linear piezoelectric polarization \vec{P}_1 is equal to :

$$\vec{P}_1 = 2e_{14} \left[\sin(2\varphi) \epsilon_{rz} \vec{u}_r + \cos(2\varphi) \epsilon_{rz} \vec{u}_\varphi + \frac{\sin(2\varphi)}{2} (\epsilon_{rr} - \epsilon_{\varphi\varphi}) \vec{u}_z \right]. \quad \text{The piezoelectric}$$

potential obtained after solving the Poisson equation, is applied as a perturbation to the $F_z = \pm 1/2$ CB and $F_z = \pm 3/2$ CB first excited states. The amplitude of the piezoelectric potential is small for the InAs/InP QD. The resulting states (figures 4-c and 4-d) show only a small deviation from the cylindrical symmetry. The perturbation was then applied to the same states in the InAs/GaAs QD. The C_{2v} symmetry clearly appears on figures 4-e and 4-f. This is due to the smaller $E_{F_z=\pm 3/2} - E_{F_z=\pm 1/2}$ splitting but also to a larger piezoelectric field. This conclusion is not modified for this QD by the inclusion of the second order piezoelectric potential [10]. Within our semi-analytical approach, a simple expression is also obtained for the polarization related to this component :

$$\vec{P}_2 = \begin{cases} \sin(2\varphi) [2B_{114} (\epsilon_{rr} + \epsilon_{\varphi\varphi}) \epsilon_{rz} + 2B_{124} (\epsilon_{rr} + \epsilon_{\varphi\varphi} + \epsilon_{zz}) \epsilon_{rz} + 2B_{156} (\epsilon_{rr} - \epsilon_{\varphi\varphi}) \epsilon_{rz}] \vec{u}_r \\ \cos(2\varphi) [2B_{114} \epsilon_{\varphi\varphi} \epsilon_{rz} + 2B_{124} (\epsilon_{rr} + \epsilon_{zz}) \epsilon_{rz}] \vec{u}_\varphi \\ \sin(2\varphi) [B_{114} (\epsilon_{rr} - \epsilon_{\varphi\varphi}) \epsilon_{zz} + B_{124} (\epsilon_{rr}^2 - \epsilon_{\varphi\varphi}^2) + 2B_{156} \epsilon_{rz}^2] \vec{u}_z \end{cases}$$

In previous study [10], it was shown that, in QD with $C_{\infty v}$ geometry, a splitting of the electronic P states result either from an interface effect [10], a relaxation via the valence force field method [7,9,10] or a piezoelectric effect [7,9,10], whereas continuum mechanics associated to effective mass models produces a vanishing splitting [13]. We show here that, in addition, there is a non-vanishing splitting due to the coupling with VB bands. This splitting which clearly appears here, because a continuum method and symmetry adapted functions are used, is however small, particularly in the InAs/GaAs system. We have shown also by comparison to our previous study [9] that accurate results can be obtained for InAs/InP QD, by introducing a few new approximations to the strained 8x8 Hamiltonian.

References

- [1] T. B. Bahder, Phys. Rev. B **41**, 11992 (1990).
- [2] P. Enders and M. Woerner, Semicond. Sci. Technol. **11**, 983 (1996).
- [3] CalvinYi-Ping Chao and S. L. Chuang, Phys. Rev. B **46**, 4110 (1992).
- [4] Y. M. Mu and S. S. Pei, J. Appl. Phys. **96**, 1866 (2004).
- [5] K. J. Vahala and P. C. Sercel, Phys. Rev. Lett. **65**, 239 (1990).
- [6] P. C. Sercel and K. J. Vahala, Phys. Rev. B **42**, 3690 (1990).
- [7] O. Stier, M. Grundmann and D. Bimberg, Phys. Rev. B **59**, 5688 (1999).
- [8] C. Pryor, Phys. Rev. B **57**, 7190 (1998).
- [9] C. Cornet, A. Schliwa, J. Even, F. Dore, C. Celebi, A. Letoublon, E. Mace, C. Paranthoen, A. Simon, P. M. Koenraad, N. Bertru, D. Bimberg and S. Loualiche, Phys. Rev. B **74**, 035312 (2006).
- [10] G..Bester and A. Zunger, Phys. Rev. B **71**, 045318 (2005).
- [11] M. Tadic, F.M. Peeters and K. L. Janssens, Phys. Rev. B **65**, 165333 (2002).
- [12] Femlab 2.0 software, Trademark of Comsol AB (2000).

- [13] P. Miska, J. Even, C. Paranthoen, O. Dehaese, A. Jibeli, M. Senes, X. Marie, Appl. Phys. Lett. **86**, 111905 (2005).
- [14] C. Cornet, M. Hayne, P. Caroff, C. Levallois, L. Joulaud, E. Homeyer, C. Paranthoen, J. Even, C. Labbe, H. Folliot, V. V. Moshchalkov and S. Loualiche, Phys. Rev. B **74**, 245315 (2006).
- [15] C. Cornet, F. Dore, A. Ballestar, J. Even, N. Bertru, A. Le Corre et S. Loualiche, J. Appl. Phys. **98**, 126105 (2005).
- [16] N. Vukmirovic, D. Indjin, V. D. Jovanovic, Z. Ikonic and P. Harrison, Phys. Rev. B **72**, 075356 (2005).

Figure captions

Figure 1 : Comparison between the CB a) and valence band (VB) b) states close to the band gap, in the 1-band representation on the left and in the axial 8-band representation on the right. The CB and VB ground states are associated respectively to $F_z = \pm 1/2$ and $F_z = \pm 3/2$. The degeneracies of CB and VB first excited states in the 1-band representation (“CB 1P” and “HH 1P”) are lifted by the coupling to remote bands.

Figure 2 : a) Variation of the gap energy as a function of the truncation height (TH) for an InAs/InP QD.

b) Variations of the hydrostatic strain $\varepsilon_{hydro} = \varepsilon_{rr} + \varepsilon_{\phi\phi} + \varepsilon_{zz}$ (dotted line) and the biaxial strain $\varepsilon_{biaxial} = \varepsilon_{rr} + \varepsilon_{\phi\phi} - 2\varepsilon_{zz}$ (straight line) along a vertical line passing through the center of a full cone.

Figure 3 : a) Variations of the “CB 1S”-“CB 1P” (straight line) and “HH 1S”-“HH 1P” (dotted line) energy gaps as a function of the truncation height for an InAs/InP QD.

b) Variation of the CB and VB first excited state splittings, $E_{F_z=\pm 3/2} - E_{F_z=\pm 1/2}$ (straight line) and $E_{F_z=\pm 1/2} - E_{F_z=\pm 5/2}$ (dotted line), as a function of the truncation height for an InAs/InP QD.

Figure 4 : Comparison between the InAs/InP and the InAs/GaAs system with the same QD geometry (TH=2.9nm). The isodensity surfaces containing 75% of the total density are shown for the $F_z = \pm 1/2$ CB ground state a) and the $F_z = \pm 1/2$ CB first excited state b) in the InAs/InP QD. Isodensity surfaces containing 75% of the total density for the eigenstates c) and d) obtained after applying the piezoelectric potential as a perturbation to the $F_z = \pm 1/2$ CB and $F_z = \pm 3/2$ CB first excited states in the InAs/InP QD. The same result is presented (e) and f)) for the InAs/GaAs QD.

FIG. 1.

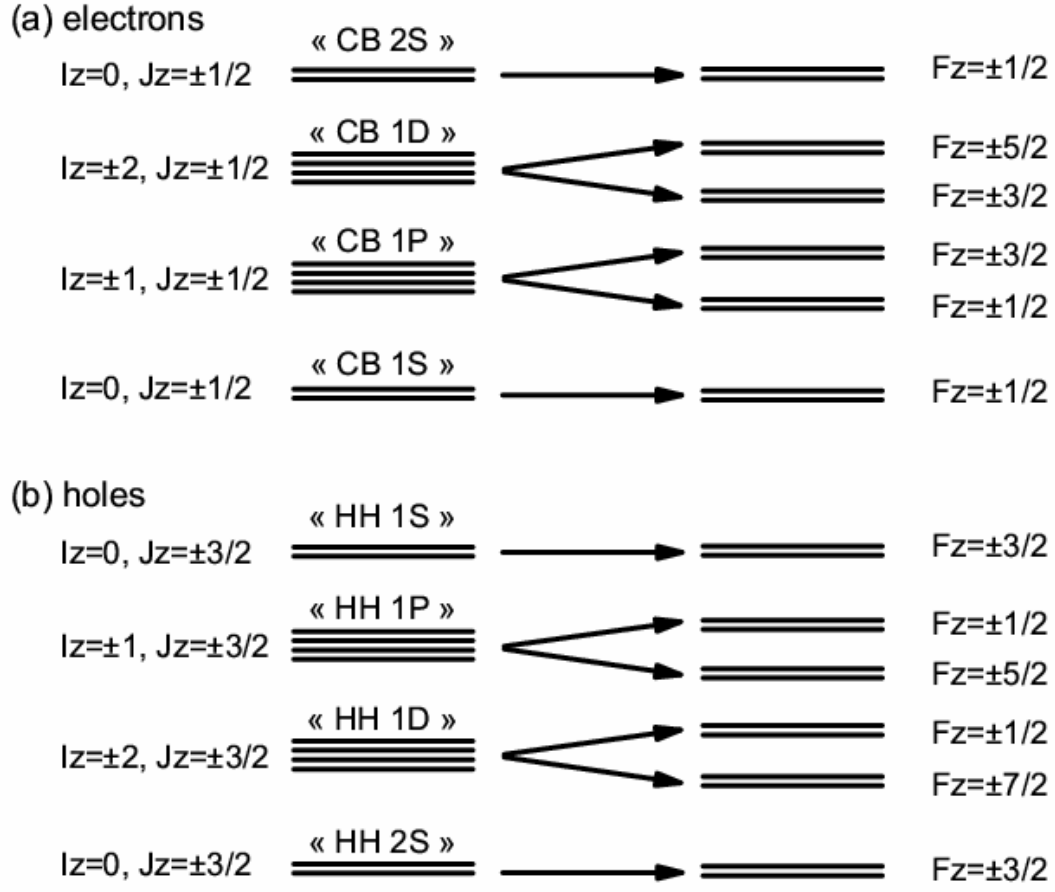
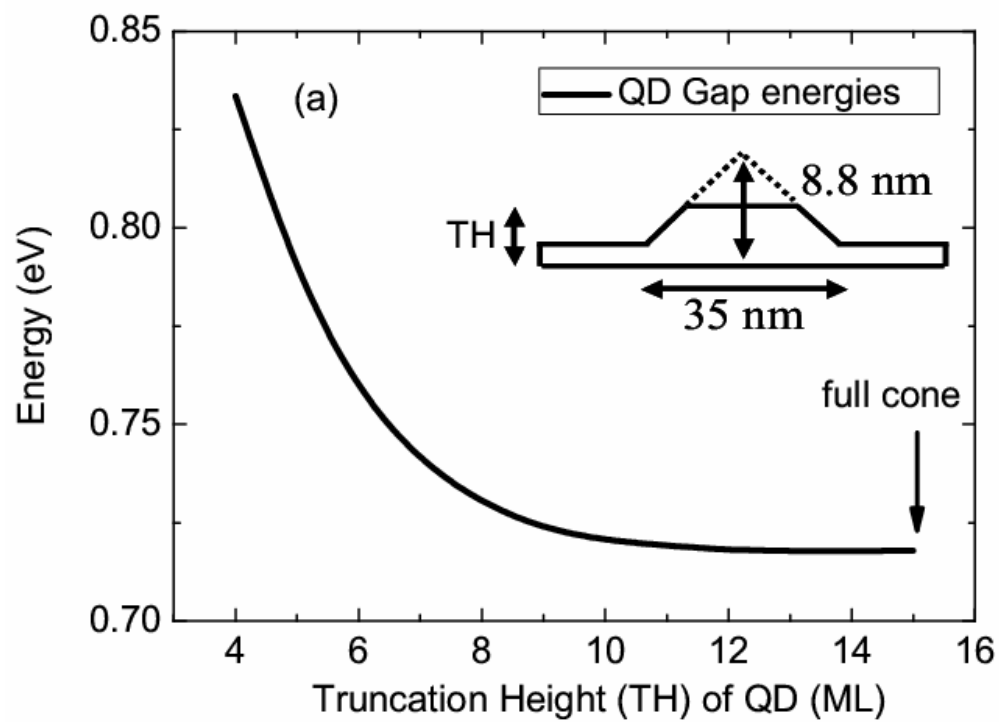


FIG. 2.

a)



(b)

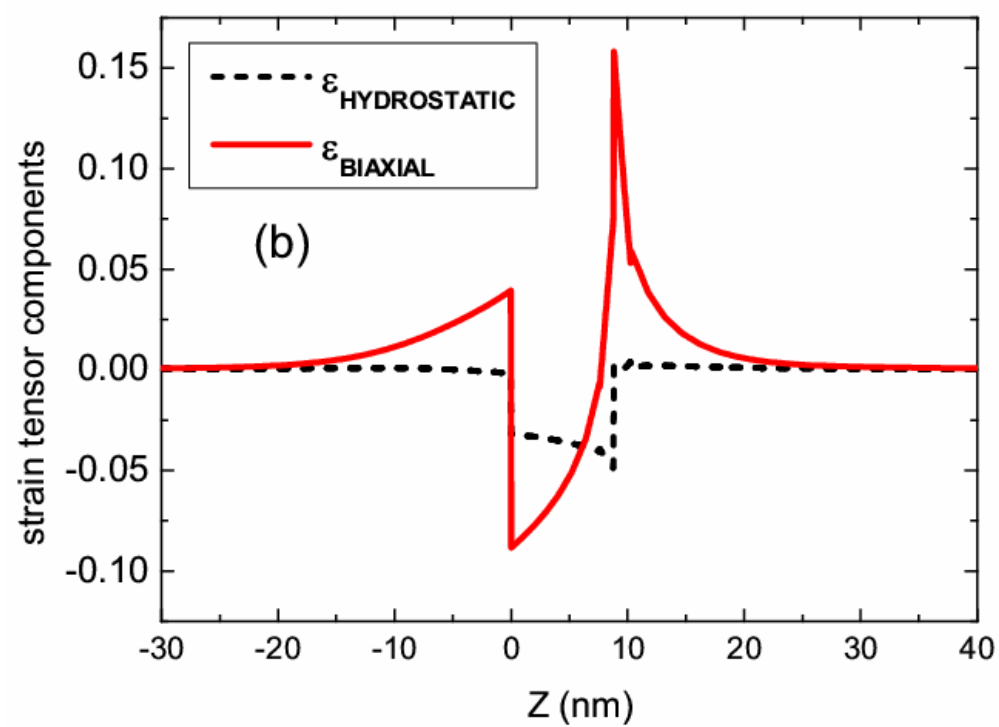


FIG. 3.

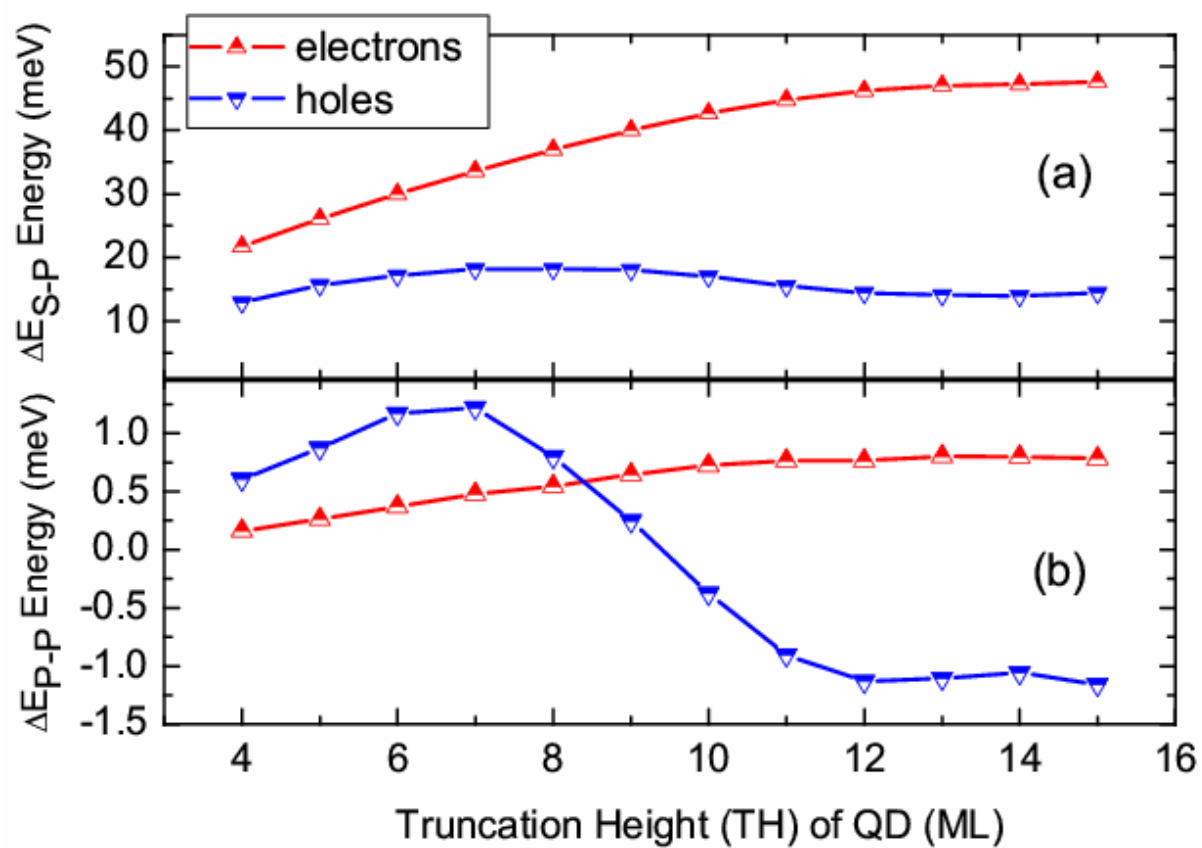
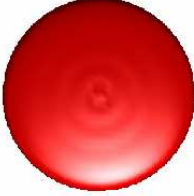


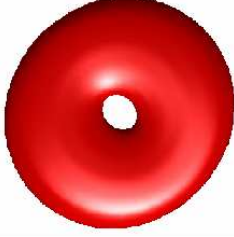
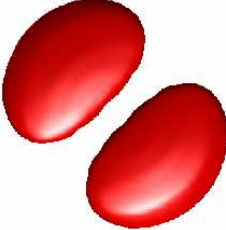


FIG. 4.

	CB ground state	CB excited state
InAs/InP QD, without piezo	(a) $F_z = \pm 1/2$ 	(b) $F_z = \pm 1/2$ 
	CB first and second excited states	
InAs/InP QD, with piezo	(c) $F_z = \pm 1/2$ 	(d) $F_z = \pm 3/2$ 
InAs/GaAs QD, with piezo	(e) $F_z = \pm 1/2$ 	(f) $F_z = \pm 3/2$ 